Springer Proceedings in Mathematics & Statistics

Angela Slavova *Editor*

New Trends in the Applications of Differential Equations in Sciences

NTADES 2025, Saints Constantine and Helena, Bulgaria, September 1–4

Springer

Springer Proceedings in Mathematics & Statistics

Volume 533

This book series features volumes composed of selected contributions from workshops and conferences in all areas of current research in mathematics and statistics, including data science, operations research and optimization. In addition to an overall evaluation of the interest, scientific quality, and timeliness of each proposal at the hands of the publisher, individual contributions are all refereed to the high quality standards of leading journals in the field. Thus, this series provides the research community with well-edited, authoritative reports on developments in the most exciting areas of mathematical and statistical research today.

Angela Slavova
Editor

New Trends in the Applications of Differential Equations in Sciences

NTADES 2025, Saints Constantine and Helena, Bulgaria, September 1–4

Springer

Editor
Angela Slavova
Institute of Mechanics, Block 4
Bulgarian Academy of Sciences
Sofia, Bulgaria

International Conference on New Trends in the Applications of Differential Equations in Sciences ntades ntades2025 NTADES 12 Saints Contantine and Helena Bulgaria 2025 09 01 2025 09 04 https://ntades.eu

ISSN 2194-1009 ISSN 2194-1017 (electronic)
Springer Proceedings in Mathematics & Statistics
ISBN 978-3-032-17070-5 ISBN 978-3-032-17071-2 (eBook)
https://doi.org/10.1007/978-3-032-17071-2

Mathematics Subject Classification: 34A37, 35C08, 35Qxx, 35Q55, 35Q92, 65-XX, 34A60, 35Q35, 60Hxx, 92D30, 34A08, 35J10, 60Gxx, 65C05, 65Mxx, 92Bxx, 92B20

© The Editor(s) (if applicable) and The Author(s), under exclusive license to Springer Nature Switzerland AG 2026

This work is subject to copyright. All rights are solely and exclusively licensed by the Publisher, whether the whole or part of the material is concerned, specifically the rights of translation, reprinting, reuse of illustrations, recitation, broadcasting, reproduction on microfilms or in any other physical way, and transmission or information storage and retrieval, electronic adaptation, computer software, or by similar or dissimilar methodology now known or hereafter developed.
The use of general descriptive names, registered names, trademarks, service marks, etc. in this publication does not imply, even in the absence of a specific statement, that such names are exempt from the relevant protective laws and regulations and therefore free for general use.
The publisher, the authors and the editors are safe to assume that the advice and information in this book are believed to be true and accurate at the date of publication. Neither the publisher nor the authors or the editors give a warranty, expressed or implied, with respect to the material contained herein or for any errors or omissions that may have been made. The publisher remains neutral with regard to jurisdictional claims in published maps and institutional affiliations.

This Springer imprint is published by the registered company Springer Nature Switzerland AG
The registered company address is: Gewerbestrasse 11, 6330 Cham, Switzerland

If disposing of this product, please recycle the paper.

Contents

Part I Applications in Mathematical Physics

Weighted Resolvent Estimates for Laplace Operator with Point Interactions 3
Vladimir Georgiev and Mario Rastrelli

Cauchy Problem for Nonlocal Parabolic PDEs 11
Petar Popivanov and Angela Slavova

From Lipschitz to One-Sided Lipschitz 39
Tzanko Donchev, Boyana Garkova, Nikolay Kitanov, Iveta Nikolova, and Stanislava Stoilova

Short Overview of the Advances in the SEsM Methodology for Obtaining Exact Solutions of Nonlinear Differential Equations 49
Zlatinka I. Dimitrova

Simulation of Local Characteristics on Flow, Heat Transfer, and Electrostatics, Using Potentials by Analytic Functions 61
Yoshihiro Mochimaru

Exact Solution to a Model Equation for Shallow-Water Waves 71
Kaloyan N. Vitanov

Localized Traveling Waves in a Spatiotemporal Population Interaction Model 83
Ivan P. Jordanov

Investigation of Fire Wave Dynamics in Forest Ecosystems via a Hyperbolic Advection–Reaction–Diffusion Equation. Part I: Analytical Solutions 93
Elena V. Nikolova, Tsvetomir Ch. Pavlov, and Gergana N. Nikolova

Travelling Wave Solutions for a Two-Species Competitive Model in Ecology 107
Teodor Georgiev and Julia Chaparova

Explicit Formulae to the Solutions of the Cauchy Problem for Schrödinger-Type Linear PDEs Depending on Small Parameter 119
Petar Popivanov and Angela Slavova

Application of Ordinary Differential Equations for Modeling the Cutting Process in Robotic Harvesting of Fruits and Vegetables..... 135
Vladimir Kotev, Ivan Ivanov, Georgi Stanchev, Jing Hu, and Georgi Komitov

Exact Solutions of Another Model Equation for Shallow-Water Waves ... 145
Kaloyan N. Vitanov

Part II Applications in Mathematical Biology and Social Sciences

On the Mathematical Theory of Popularity Waves Based on the SIIRR Model of Epidemic Spread..... 161
Nikolay K. Vitanov

Wavetrains of Popularity Waves Based on the SIIRR Model of Epidemic Spread 171
Nikolay K. Vitanov

Overview of the Recent Applications of the Simple Equations Method (SEsM) to Problems of Epidemic Spread and Social Dynamics .. 181
Zlatinka I. Dimitrova

Modeling the Trajectories of Bloodstain on the Crime Scene, Using Mathematical Reconstruction Method 191
Georgi Georgiev, Slavi Georgiev, and Katina Kisyova

Mathematical Estimation of Pig Body Volume from Longitudinal Width Profiles 203
Vladimir K. Kotev, Ivan P. Jordanov, Ivan S. Ivanov, Ivelina Zapryanova, Jing Hu, Bilyana S. Stoynova, and Georgi B. Ivanov

Part III Applications in Numerical Analysis and Computer Science

Minimizing Gauss Quadrature Error Estimates by a New Taylor-Like Formula..... 215
Joel Chaskalovic and Franck Assous

Efficient Solution of Fisher's and Huxley's Equations: Comparisons of Stable Explicit and Implicit Finite-Difference Methods 225
Husniddin Khayrullaev and Endre Kovács

Effective Stochastic Techniques for Solving Linear Algebraic Systems 239
Venelin Todorov, Slavi Georgiev, Stoyan Apostolov, Yuri Dimitrov, Velichka Traneva, and Stoyan Tranev

Robust Unbiased Monte Carlo Methods for High-Dimensional Fredholm Integral Equations 251
Venelin Todorov, Slavi Georgiev, Stoyan Apostolov, and Fatima Sapundzhi

Precise Computation of Solutions to Third-Order Nonlinear Dispersive Equations 263
Miglena N. Koleva and Lubin G. Vulkov

Refined Monte Carlo Strategies for Solving Multidimensional Integrals in Statistics 275
Venelin Todorov

An Advanced Lattice-Based Strategy for High-Dimensional Sensitivity Study 287
Venelin Todorov

Investigation of Fire Wave Dynamics in Forest Ecosystems via a Hyperbolic Advection-Reaction-Diffusion Equation. Part II. Numerical Investigation 299
Gergana N. Nikolova, Tsvetomir Ch. Pavlov, and Elena V. Nikolova

Design and Implementation of a Numerical Model for Environmental Applications 311
Tzvetan Ostromsky, Silvi-Maria Gurova, Meglena Lazarova, and Venelin Todorov

Part IV Applications in Financial Mathematics

Finite Element Solution of the Two-Dimensional Bates Model for Option Pricing Under Stochastic Volatility and Jumps 325
Neda Bagheri Renani and Daniel Ševčovič

Enhanced Monte Carlo Techniques for Pricing High-Dimensional European Options 337
Venelin Todorov, Stoyan Apostolov, Mirosav Stoenchev, Yuri Dimitrov, and Fatima Sapundzhi

Studying the Impact of Foreign Direct Investments on Bulgaria's Economic Growth by Sectors 349
Vesela Mihova, Debora Marinova, and Velizar Pavlov

Granularity Adjustment for the Inferred-Loss-Rate-Based Estimate of the Capital Adequacy Threshold 361
Vilislav Boutchaktchiev

A Study of the Relationship Between Education and Median Income in Bulgaria 371
Vesela Mihova, Monika Deneva, and Velizar Pavlov

Optimized Algorithmic Grid Strategy Trading in Cryptomarkets 385
Svetoslav Hadzhiivanov, Slavi Georgiev, Borislav Chakarov, Juri Kandilarov, and Venelin Todorov

Computational Recovery of Time-Dependent Volatility of Fixed Strike Asian Option from Integral Premium Observations 397
Slavi Georgiev and Lubin Vulkov

Forecasting and Modelling of the FAO Food Price Index Time Series 409
Slavi Georgiev and Byulent Idirizov

Option Premium Modeling via Stochastic Approaches 421
Teodora Klimenko and Velizar Pavlov

The Comparison Between the 2024 Forecast for the RBNS Reserve and the Actual 2024 Data, along with their Deviations 433
Marina Gospodinova, Elitsa Raeva, and Velizar Pavlov

Part V Applications in Fractional Analysis

Ulam Stability of Impulsive Caputo-Type Fractional Differential Equations and Boundary Conditions 445
Snezhana Hristova

Boundedness and Lagrange Stability Criteria of Perturbed Impulsive Differential Equations With Respect to Its Unperturbed One With an Initial Time Difference 455
Saliha Demirbüken and Coşkun Yakar

Analysis of an Inverse Tempered Fractional Stationary Problem on Disjoint Intervals 467
Miglena N. Koleva and Lubin G. Vulkov

Semilinear Functional Evolution Inclusions 479
Tzanko Donchev, Boyana Garkova, Nikolay Kitanov, Iveta Nikolova, and Stanislava Stoilova

Fractional Approach to the Study of the Green's Function for Some Relevant Time-Space Partial Differential Equation of Mathematical Physics 489
Fernando Olivar-Romero

Finite Time Stability for Delay Fractional Differential Equations with Caputo Fractional Derivative With Respect to Another Function 501
Snezhana Hristova

Part VI Applications in Neural Networks and Artificial Intelligence

Artificial Intelligence for Studying Traveling Wave Solutions of Several Mathematical Physics Equations 513
Angela Slavova and Ventsislav Ignatov

Neural Network Ensembles for Financial Forecasting and Portfolio Optimization 525
Maya Markova

Physics-Informed Neural Networks for Studying Nonlinear Schrödinger Equation 541
Angela Slavova and Taim Saker

Finite Element Solution of the Two-Dimensional Bates Model for Option Pricing Under Stochastic Volatility and Jumps



Neda Bagheri Renani and Daniel Ševčovič

Abstract We propose a fourth-order compact finite-difference (HOC-FD) scheme for the transformed Bates partial integrodifferential equation (PIDE). The method employs an implicit-explicit (IMEX) Crank-Nicolson framework for local terms and Simpson quadrature for the jump integral. Benchmarks against second-order finite differences (FD) and quadratic finite elements (FEM, $p = 2$) confirm near-fourth-order spatial accuracy for HOC-FD, near second order for FEM, and second-order temporal convergence for all time integrators. Efficiency tests show that HOC-FD achieves similar accuracy at up to two orders of magnitude lower runtime than FEM, establishing it as a practical baseline for option pricing under stochastic volatility jump-diffusion models.

Keywords Bates model · Option pricing · Partial integrodifferential equation (PIDE) · High-order compact finite difference · Finite element method

1 Introduction

Stochastic volatility models with jumps, such as the Bates model, lead to partial integrodifferential equations (PIDEs) central to option pricing. Their complexity motivates efficient high-order numerical solvers [8, 9]. Compact high-order finite difference schemes have been successfully applied to liquidity shock models [15], nonlinear PDEs [13], fractional extensions [10], and uncertain correlation problems [14], confirming their advantages for accuracy and stability.

We develop a fourth-order compact finite-difference (HOC-FD) scheme for the transformed Bates PIDE, combining an IMEX-Crank-Nicolson split for local terms with Simpson quadrature for the jump integral. Benchmarks against second-order

N. Bagheri Renani (✉) · D. Ševčovič
Department of Applied Mathematics and Statistics, Comenius University in Bratislava, Bratislava, Slovakia
e-mail: neda.bagheri@fmph.uniba.sk; sevcovic@fmph.uniba.sk

© The Author(s), under exclusive license to Springer Nature Switzerland AG 2026

A. Slavova (ed.), *New Trends in the Applications of Differential Equations in Sciences*, Springer Proceedings in Mathematics & Statistics 533,
https://doi.org/10.1007/978-3-032-17071-2_27

finite differences and quadratic FEM demonstrate near fourth-order spatial accuracy, second-order temporal accuracy, and substantial efficiency gains, establishing HOC-FD as a competitive baseline for option pricing under stochastic volatility jump-diffusion models.

2 Stochastic Differential Equations of the Bates Model

The Bates model augments the Heston stochastic-volatility framework with a jump component in the asset price, combining continuous variance dynamics with discontinuous returns to better reproduce market skew, fat tails, and smile effects ([2, 6, 23] see also [9]).

Risk-neutral dynamics. Let $S(t)$ denote the price of the asset and $v(t)$ the variance. Under the risk-neutral measure with correlation ρ between Brownian drivers

$$dS(t) = \mu S(t)dt + \sqrt{v(t)}S(t)dW_S(t) + S(t)dJ(t),$$

$$dv(t) = \kappa(\theta - v(t))dt + \sigma\sqrt{v(t)}dW_v(t),$$

where $\kappa > 0$ (mean-reversion speed), $\theta > 0$ (long-run variance), and $\sigma > 0$ (volatility of variance). The jump process $J(t)$ is Poisson with intensity λ; logarithmic jump sizes Y are often modeled Gaussian with mean μ_J and variance σ_J^2, yielding multiplicative price jumps $S \mapsto Se^Y$ [11, 19].

Option-pricing PIDE. For an option value $V(S, v, t)$ with a risk-free rate r, the price satisfies the partial integrodifferential equation:

$$\frac{\partial V}{\partial t} + \frac{1}{2}S^2 v\frac{\partial^2 V}{\partial S^2} + \rho\sigma v S\frac{\partial^2 V}{\partial S\partial v} + \frac{1}{2}\sigma^2 v\frac{\partial^2 V}{\partial v^2} + (r-\lambda)S\frac{\partial V}{\partial S} + \kappa(\theta - v)\frac{\partial V}{\partial v}$$
$$- (r+\lambda)V = \lambda\int_{\mathbb{R}}\left[V(Se^z, v, t) - V(S, v, t) - \left(e^z - 1\right)S\frac{\partial V}{\partial S}(S, v, t)\right]f(z)\,dz.$$

where $f(z)$ is the density of the log-jump size z (e.g., Gaussian with mean μ_J and variance σ_J^2) and where $f(z)$ denotes the density of the log jump size z (typically $z \sim \mathcal{N}(\mu_J, \sigma_J^2)$) [4, 5].

2.1 Transformed Bates Model PIDE

To obtain a numerically convenient form, we introduce the backward time and normalized variables:

$$\tau = T - t \qquad x = \ln \frac{S}{K} \qquad y = \frac{\sigma}{v} \qquad u(x, y, \tau) = \frac{1}{K}\, e^{(r+\lambda)\tau}\, V(S, v, t).$$

Here, K is the strike, r the risk-free rate, and the parameter $\lambda > 0$ measures the intensity of jumps. Let $f(z)$ denote the probability density of the logarithmic jump size [11, 20]. With these variables and using differentiation rules, we have

$$S\frac{\partial}{\partial S} = \frac{\partial}{\partial x},\ v\frac{\partial}{\partial v} = -y\frac{\partial}{\partial y},\ S^2\frac{\partial^2}{\partial S^2} = \frac{\partial^2}{\partial x^2} - \frac{\partial}{\partial x},\ v\frac{\partial}{\partial v} = -y\frac{\partial}{\partial y},$$

$$v\frac{\partial^2}{\partial v^2} = \frac{y^3}{\sigma}\frac{\partial^2}{\partial y^2} + 2\frac{y^2}{\sigma}\frac{\partial}{\partial y},\ vS\frac{\partial^2}{\partial S \partial v} = -y\frac{\partial^2}{\partial x \partial y},$$

$$\frac{\partial V}{\partial t} - (r+\lambda)V = -K\, e^{-(r+\lambda)\tau}\frac{\partial u}{\partial \tau},\quad V(Se^z, v, t) = K\, e^{-(r+\lambda)\tau} u(x+z, y, \tau).$$

Thus, the transformed PIDE reads as follows:

$$\begin{aligned} &-\frac{\partial u}{\partial \tau} + \frac{\sigma}{2y}\left(\frac{\partial^2 u}{\partial x^2} - \frac{\partial u}{\partial x}\right) - \rho\sigma y \frac{\partial^2 u}{\partial x \partial y} + \frac{\sigma}{2}\left(y^3\frac{\partial^2 u}{\partial y^2} + 2y^2\frac{\partial u}{\partial y}\right) \\ &+ (r-\lambda)\frac{\partial u}{\partial x} - \kappa\left(\theta - \frac{\sigma}{y}\right)\frac{y^2}{\sigma}\frac{\partial u}{\partial y} \\ &+ \lambda \int_{\mathbb{R}} \left[u(x+z, y, \tau) - u(x, y, \tau) - \left(e^z - 1\right)\frac{\partial u}{\partial x}(x, y, \tau)\right] f(z)\, dz = 0. \end{aligned} \tag{1}$$

3 Spatial Discretization and IMEX-Crank-Nicolson

We consider a uniform tensor product grid $\{(x_i, y_j) : i = 0, \ldots, N_x,\ j = 0, \ldots, N_y\}$, $x_i = x_{\min} + i\, h_x$, $y_j = y_{\min} + j\, h_y$, with spatial discretization steps $h_x, h_y > 0$. Let $u_{i,j}^n$ denote the approximation to $u(x_i, y_j, \tau_n)$ at time levels $\tau_n = nk$, where $k = T/N_\tau$. The center difference operators D_x, D_y, D_{xx}, D_{yy}, D_{xy} will be used for the spatial derivatives (their concrete stencils are given in Sects. 3.1–3.2). The local (differential) part of (1) reads as

$$L[u] = \frac{\sigma}{2y}u_{xx} + \frac{\sigma}{2}y^3 u_{yy} - \rho\sigma y\, u_{xy} + \left(r - \lambda - \frac{\sigma}{2y}\right)u_x + \left(\sigma y^2 + \kappa y - \kappa\theta\frac{y^2}{\sigma}\right)u_y.$$

Its discrete counterpart at (x_i, y_j) is

$$L_h[u]_{i,j} = \frac{\sigma}{2y_j} D_{xx}u + \frac{\sigma}{2}y_j^3\, D_{yy}u - \rho\sigma y_j\, D_{xy}u + \left(r - \lambda - \frac{\sigma}{2y_j}\right)D_x u$$

$$+\left(\sigma y_j^2+\kappa y_j-\kappa\theta\frac{y_j^2}{\sigma}\right)D_y u.$$

The nonlocal (jump) term in (1) is treated explicitly. Its discrete approximation $I_h[u]_{i,j}$ is designed to match the integral part in (1):

$$I_h[u]_{i,j}=\lambda\int_{\mathbb{R}}\big(u(x_i+z,y_j,\tau)-u(x_i,y_j,\tau)-(e^z-1)\,u_x(x_i,y_j,\tau)\big)f(z)\,dz.$$

With these definitions, the semi-discrete system has the form:

$$\frac{du}{d\tau}u=L_h[u]+I_h[u].$$

For time stepping, we use an IMEX-Crank-Nicolson scheme: the local operator L_h is treated implicitly and the jump operator I_h explicitly. Writing U^n for the vector of all grid values at time τ_n, one step from n to $n+1$ is given by

$$\frac{U^{n+1}-U^n}{k}=\frac{1}{2}L_h[U^{n+1}+U^n]+I_h[U^n].$$

Sections 3.1 and 3.2 provide the compact spatial stencils for L_h and the quadrature/convolution realization of I_h, respectively (cf. [4, 11, 23]).

3.1 Fourth-Order Compact Discretization of the Local Operator

We denote $u_{i,j}\approx u(x_i,y_j,\tau)$ and adopt fourth-order compact relations to approximate first-, second-, and mixed derivatives on a 3×3 stencil. Such compact schemes are well established for elliptic and parabolic PDEs with variable coefficients and are known for their spectral-like resolution [11, 17, 21, 22].

Compact line relations (1D, fourth order). For fixed j (differentiation in x)

$$\tfrac{1}{4}u_{x,i-1,j}+u_{x,i,j}+\tfrac{1}{4}u_{x,i+1,j}=\frac{u_{i+1,j}-u_{i-1,j}}{2h_x},\tag{2}$$

$$\tfrac{1}{12}u_{xx,i-1,j}+\tfrac{10}{12}u_{xx,i,j}+\tfrac{1}{12}u_{xx,i+1,j}=\frac{u_{i-1,j}-2u_{i,j}+u_{i+1,j}}{h_x^2}.\tag{3}$$

For fixed i (differentiation in y)

$$\tfrac{1}{4}u_{y,i,j-1}+u_{y,i,j}+\tfrac{1}{4}u_{y,i,j+1}=\frac{u_{i,j+1}-u_{i,j-1}}{2h_y},\tag{4}$$

$$\tfrac{1}{12}u_{yy,i,j-1} + \tfrac{10}{12}u_{yy,i,j} + \tfrac{1}{12}u_{yy,i,j+1} = \frac{u_{i,j-1} - 2u_{i,j} + u_{i,j+1}}{h_y^2}. \tag{5}$$

Mixed derivative via sequential compact differentiation. Let $M_x = \mathrm{tridiag}(\frac{1}{4}, 1, \frac{1}{4})$ and D_x the centered difference line operator in x, with M_y, D_y defined analogously. The mixed derivative is evaluated by

$$U_{xy} = M_x^{-1} D_x \big(M_y^{-1} D_y U\big) = M_y^{-1} D_y \big(M_x^{-1} D_x U\big).$$

Compact local operator (nodewise form). With coefficients taken directly from the transformed Bates operator (1), we have

$$(L_h[U])_{i,j} = a_{i,j}U_{xx} + b_{i,j}U_{yy} + c_{i,j}U_{xy} + d_{i,j}U_x + e_{i,j}U_y + f_{i,j}U_{i,j}, \tag{6}$$

where

$$a_{i,j} = \frac{1}{2}\frac{\sigma}{y_j}, \quad b_{i,j} = \frac{1}{2}\sigma y_j^3, \quad c_{i,j} = -\rho\sigma y_j, \quad d_{i,j} = (r-\lambda) - \frac{1}{2}\frac{\sigma}{y_j},$$

$$e_{i,j} = \sigma y_j^2 + \kappa y_j - \kappa\theta\frac{y_j^2}{\sigma}, \quad f_{i,j} = 0.$$

Here, $U_x, U_y, U_{xx}, U_{yy}, U_{xy}$ are supplied by the compact relations (2)–(5) and the mixed construction above. The interior accuracy satisfies

$$L_h[u] - L[u] = O(h_x^4 + h_y^4).$$

Nine-point compact balance (assembled stencil). Eliminating auxiliary derivatives from (2)–(5) within (6) yields a 3×3 balance:

$$\sum_{\ell=0}^{8} \alpha_\ell u_\ell = \sum_{\ell=0}^{8} \gamma_\ell f_\ell,$$

with $\{u_\ell\}$ the stencil values centered at (i, j) and $\{f_\ell\}$ the right-hand side samples (arising from PDE insertion at (i, j)). The weights α_ℓ, γ_ℓ depend only on the local coefficients and (h_x, h_y).

Verification template (constant coefficients). For $a = b = 1$, $c = d = e = 0$, $h_x = h_y = h$, the scheme reduces to the classical fourth-order nine-point Laplacian [1, 7]:

$$\frac{-u_{i-1,j-1} + 16u_{i,j-1} - u_{i+1,j-1} + 16u_{i-1,j} - 60u_{i,j} + 16u_{i+1,j}}{12h^2}$$

$$+ \frac{-u_{i-1,j+1} + 16u_{i,j+1} - u_{i+1,j+1}}{12h^2} = f_{i,j} + \tfrac{h^2}{12}\,\Delta f_{i,j}.$$

providing a convenient code check in line with established compact formulations for financial PIDEs [2, 3, 11, 12, 18].

3.2 Nonlocal Jump Operator and IMEX-CN Time Marching

The nonlocal jump part of (1) is

$$\lambda \int_{\mathbb{R}} \big[u(x+z,y,\tau) - u(x,y,\tau) - (e^z-1)u_x(x,y,\tau)\big] f(z)\,dz,$$

with lognormal jump density $f(z)$ [5, 7, 19]. The compensator $(e^z-1)u_x$ guarantees integrability and preserves the martingale condition.

Discrete jump operator. On the grid, we approximate

$$(I_h[u])_{i,j} = \lambda \sum_{m=-M}^{M} \omega_m \big[u(x_i+z_m, y_j, \tau) - u(x_i, y_j, \tau) - (e^{z_m}-1) D_x u(x_i, y_j, \tau)\big],$$

using quadrature nodes $\{z_m\}$ and weights $\{\omega_m\}$, with interpolation for off-grid values [7, 11, 18].

IMEX-CN scheme. The semi-discrete system

$$\frac{d}{d\tau} U = L_h[U] + I_h[U]$$

is advanced in time by the IMEX-Crank-Nicolson method [2, 16]:

$$\frac{U^{n+1}-U^n}{k} = \frac{1}{2} L_h[U^{n+1}+U^n] + I_h[U^n],$$

treating L_h implicitly and I_h explicitly. This combination retains unconditional stability for the stiff diffusion operator while avoiding costly implicit treatment of the integral. The scheme fits naturally into high-order compact PIDE solvers [11, 12, 21].

4 Initial and Boundary Conditions

For the transformed Bates PIDE, we prescribe the payoff as the initial condition at $\tau = 0$:

$$u(x,y,0) = \max(1-e^x, 0).$$

At the far left boundary $x_{\min}$, the option value approaches the discounted intrinsic value. Thus, we impose

$$u(x_{\min}, y, \tau) = e^{(r+\lambda)\tau}\left(1 - e^{x_{\min}}\right).$$

At the far right boundary $x_{\max}$, the put option value decays, so we set

$$u(x_{\max}, y, \tau) = 0.$$

In the variance direction, we impose homogeneous Neumann conditions:

$$\partial_y u(x, y_{\min}, \tau) = 0, \qquad \partial_y u(x, y_{\max}, \tau) = 0.$$

These conditions ensure consistency with the no-arbitrage bounds for European puts under stochastic volatility jump-diffusion dynamics.

5 Benchmarking via the Finite Element Method

We benchmark the compact finite-difference scheme against a conforming finite element method (FEM) applied to the transformed Bates PIDE under identical payoff and boundary conditions. The comparison highlights accuracy, stability, and computational cost.

Weak formulation. Writing the local operator in divergence form, we enforce economic Dirichlet conditions on vertical boundaries and homogeneous Neumann conditions on horizontal ones, consistent with the FD setup. The weak form reads

$$\left(\tfrac{u^{n+1}-u^n}{\Delta\tau}, \psi\right) + a\left(\tfrac{u^{n+1}+u^n}{2}, \psi\right) = \left(\tfrac{3}{2}L_I[u^n] - \tfrac{1}{2}L_I[u^{n-1}], \psi\right), \quad \forall \psi \in V,$$

with $V = \{\psi \in H^1(\Omega) : \psi|_{\Gamma_D} = 0\}$ and bilinear form

$$a(u, \psi) = \int_\Omega A\nabla u \cdot \nabla\psi \, dxdy + \int_\Omega (b \cdot \nabla u)\psi \, dxdy.$$

Spatial discretization. In a regular shape mesh, we use $V_h \subset V$ with continuous quadratic elements (P2/Q2). The Gaussian quadrature yields the mass M, stiffness K, and convection C matrices. For coefficient vector U^n

$$A_h U^{n+1} = B_h U^n + \Delta\tau\left(\tfrac{3}{2}F^n - \tfrac{1}{2}F^{n-1}\right),$$

with $A_h = M + \frac{\Delta\tau}{2}(K + C)$, $B_h = M - \frac{\Delta\tau}{2}(K + C)$, and $F^n = (L_I[u_h^n], \phi_i)$.

For time-independent coefficients, a sparse factorization of A_h is reused.

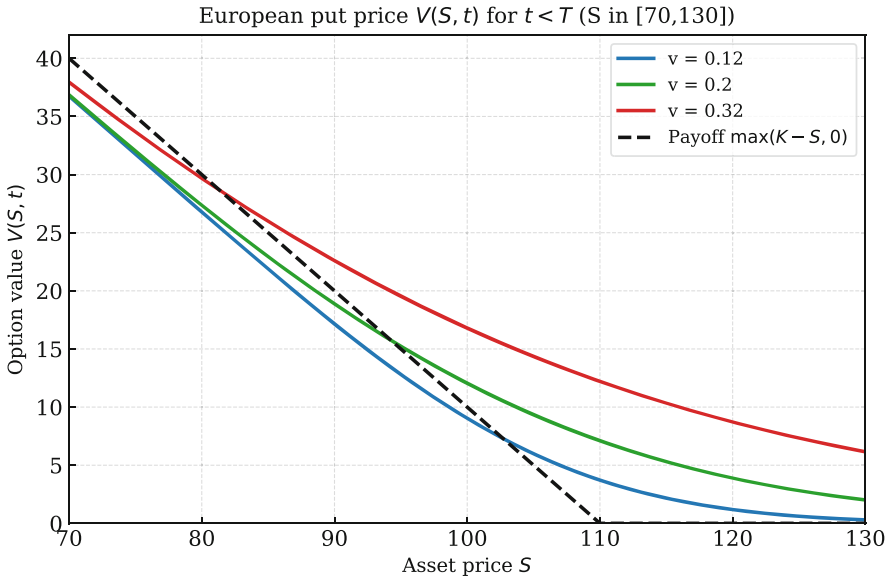


Fig. 1 European put price $V(S,t)$ under the Bates model for $S \in [70, 130]$. The intrinsic payoff $\max(K - S, 0)$ and the no-arbitrage lower bound $\max\{Ke^{-rT} - S, 0\}$ are shown as reference curves

Jump treatment. The nonlocal operator is evaluated explicitly by Simpson quadrature on a truncated log-jump interval, with FEM interpolation at off-grid x-values. This keeps the implicit system confined to local terms.

Takeaway. FEM achieves near second-order spatial convergence for quadratic elements [4, 23, 24], but in structured domains, HOC-FD attains comparable accuracy with significantly lower runtime and memory [11, 21] (Fig. 1).

6 Numerical Experiments

We evaluate the (HOC-FD) scheme for the transformed Bates PIDE against second-order finite differences and FEM with Lagrange bases of degree $p = 1, 2$. All solvers employ identical payoff and boundary conditions, the IMEX-CN scheme for local terms and explicit Simpson quadrature on a truncated interval for the jump integral (Table 1). Accuracy is measured by discrete L^2 error and RMSE relative to a high-resolution reference, while efficiency is assessed in terms of degrees of freedom, CPU time, memory usage, and a cost-accuracy ratio.

Table 1 Simulation parameters used in Bates model experiments

Parameter	Value	Parameter	Value	Parameter	Value
K	110	T (years)	1.0	r	0.03
κ	1.8	θ	0.02	ρ	-0.4
σ	0.15	λ	0.25	Jump law	Lognormal
μ_J	Set per exp.	σ_J	Set per exp.	–	–

Table 2 Observed convergence orders in space and time, comparing HOC-FD with second-order finite differences [2, 7] and FEM(P2) [4, 23, 24]. Spatial studies fix $\Delta\tau/h^2$; temporal studies fix h

Method	Spatial order p_s	Temporal order p_t
FEM (P2)	≈ 2.0 (both L^2, L^∞)	≈ 2.0 (CN, BDF2, MP)
HOC-FD (compact)	≈ 4.0 (both L^2, L^∞)	≈ 2.0 (IMEX-CN)

6.1 Numerical Convergence

We measure numerical accuracy using three error norms:

$$\|u^h - u^{ref}\|_{L^2} = \left(h_x h_y \sum_{i=1}^{N_x} \sum_{j=1}^{N_y} (u_{i,j}^h - u_{i,j}^{ref})^2 \right)^{1/2},$$

the discrete L^2 error norm, which approximates the continuous integral norm

$$\text{RMSE} = \left(\frac{1}{N_x N_y} \sum_{i=1}^{N_x} \sum_{j=1}^{N_y} (u_{i,j}^h - u_{i,j}^{ref})^2 \right)^{1/2},$$

the root mean square error, representing average nodal error, and

$$\|u^h - u^{ref}\|_{L^\infty} = \max_{1 \le i \le N_x,\, 1 \le j \le N_y} |u_{i,j}^h - u_{i,j}^{ref}|,$$

the maximum pointwise error (Table 2).

Thus, L^2 reflects global accuracy, RMSE captures average nodal error, and L^∞ highlights the worst-case deviation [2, 16, 23].

6.2 Computational Efficiency Comparison

Efficiency was assessed using the cost-accuracy ratio:

Table 3 Efficiency snapshot at $h = 0.1$ relative to HOC-FD baseline [11, 21]. Comparisons include second-order finite differences [2, 7] and FEM(P2) [4, 23, 24]. Errors measured against a high-resolution reference; η uses L^2 error and runtime

Method	DOF	Time (s)	L^2	RMSE	η
HOC-FD (IMEX-CN)	1681	1.106	0.0230	0.0095	1.00
FEM (P_2)	6561	23.426	0.1522	0.0475	$\approx 1.40 \times 10^2$
CN (second-order FD)	1681	2.230	0.0341	0.0148	≈ 2.99
BDF2 (second-order FD)	1681	2.904	0.0417	0.0181	≈ 4.76
Midpoint (FD)	1681	3.117	0.0425	0.0185	≈ 5.21

$$\eta_{A/B} = \frac{\varepsilon_A^2\, t_A}{\varepsilon_B^2\, t_B}, \qquad \varepsilon \in \{\|\cdot\|_{L^2}, \mathrm{RMSE}\},$$

reported relative to the HOC-FD baseline ($\eta = 1$). Here, t denotes CPU time.

Table 3 shows that, at matched settings, the compact HOC-FD scheme attains comparable accuracy at substantially lower runtime on structured grids. Relative to HOC-FD, FEM(P2) is roughly two orders of magnitude more costly, while second-order FD variants are within single-digit multiples of the baseline. These results confirm earlier findings that compact FD schemes achieve significant efficiency gains over FEM in structured domains [4, 11, 24].

7 Conclusion

We developed a fourth-order compact finite-difference scheme for the transformed Bates PIDE, combining an IMEX-Crank-Nicolson split for local terms with explicit Simpson quadrature for the jump integral. Benchmarks against second-order finite differences and quadratic FEM confirmed near-fourth-order spatial accuracy for the compact scheme and near second order for FEM, with all time integrators exhibiting second-order accuracy. Efficiency tests on structured grids showed that the compact scheme achieves substantially lower runtimes—up to two orders of magnitude faster than FEM—while maintaining comparable pricing accuracy. This establishes the scheme as a competitive baseline for structured-domain option pricing. Future work will extend the method to American and path-dependent payoffs, adaptive meshes, broader jump specifications, and accelerated integral solvers.

Acknowledgements The first author was supported by Comenius University grant UK/1024/2025. The second author received support from the Slovak VEGA 1-0493-24 agency.

References

1. Achdou, Y., Franchi, B., Tchou, N.: A partial differential equation connected to option pricing with stochastic volatility: regularity results and discretization. Math. Comput. **74**(251), 1291–1322 (2005)
2. Bagheri, N., Haghighi, H.K.: A comparison study of ADI and LOD methods on option pricing models. J. Math. Finance **7**(2), 275–290 (2017)
3. Balajewicz, M., Toivanen, J.: Reduced order models for pricing European and American options under stochastic volatility and jump-diffusion models. J. Comput. Sci. **20**, 198–204 (2017)
4. Ballestra, L.V., Sgarra, C.: The evaluation of American options in a stochastic volatility model with jumps: An efficient finite element approach. Comput. Math. Appl. **60**(6), 1571–1590 (2010)
5. Bates, D.S.: Jumps and stochastic volatility: Exchange rate processes implicit in Deutsche Mark options. Rev. Financ. Stud. **9**(1), 69–107 (1996)
6. Black, F., Scholes, M.: The pricing of options and corporate liabilities. J. Polit. Econ. **81**(3), 637–654 (1973)
7. Cont, R., Voltchkova, E.: A finite difference scheme for option pricing in jump diffusion and exponential Lévy models. SIAM J. Numer. Anal. **43**(4), 1596–1626 (2005)
8. Cruz, J.M.T.S., Ševčovič, D.: On solutions of a partial integro-differential equation in Bessel potential spaces with applications in option pricing models. Jpn. J. Ind. Appl. Math. **37**(3), 697–721 (2020)
9. Cruz, J.M.T.S., Ševčovič, D.: Option pricing in illiquid markets with jumps. Appl. Math. Finance **25**(4), 395–415 (2018)
10. Dimitrov, D., Vulkov, L.: High order finite difference schemes on non-uniform meshes for the time-fractional Black–Scholes equation. Appl. Numer. Math. **111**, 251–266 (2016)
11. Düring, B., Pitkin, A.: High-order compact finite difference scheme for option pricing in stochastic volatility jump models. J. Comput. Appl. Math. **355**, 201–217 (2019)
12. Düring, B., Pitkin, A.: Efficient hedging in Bates model using high-order compact finite differences. arXiv preprint arXiv:1710.05542 (2024)
13. Koleva, M.N., Vulkov, L.G.: A kernel-based algorithm for numerical solution of nonlinear PDEs in finance. In: Numerical Analysis and Its Applications (NAA 2012). Lect. Notes Comput. Sci., vol. 8236, pp. 520–527. Springer, Heidelberg (2013)
14. Koleva, M.N., Vulkov, L.G.: A positive flux limited difference scheme for option pricing 2D fully non-linear parabolic equation with uncertain correlation. J. Comput. Appl. Math. **271**, 368–382 (2014)
15. Koleva, M.N., Vulkov, L.G., Mudzimbabwe, T.: Fourth-order compact schemes for a parabolic-ordinary system of European option pricing liquidity shocks model. Numer. Algorithms **74**, 1075–1098 (2017)
16. Kreiss, H.O.: Initial boundary value problems for hyperbolic systems. Commun. Pure Appl. Math. **23**(3), 277–298 (1970)
17. Lele, S.K.: Compact finite difference schemes with spectral-like resolution. J. Comput. Phys. **103**(1), 16–42 (1992)
18. Mao, M., Tian, H., Wang, W.: A variable step-size extrapolated Crank–Nicolson method for option pricing under stochastic volatility model with jump. Math. Methods Appl. Sci. **47**(2), 762–781 (2024)
19. Merton, R.C.: Option pricing when underlying stock returns are discontinuous. J. Financ. Econ. **3**(1-2), 125–144 (1976)
20. Pankratov, E.: Nonlinear profit maximization with account changing of prices. Int. J. Model. Simul. Appl. **2**(2), 9–17 (2018)
21. Pitkin, A.: High-order compact finite difference schemes for option pricing in stochastic volatility jump-diffusion models. Ph.D. thesis, University of Sussex (2020)

22. Spotz, W.F., Carey, G.F.: A high-order compact formulation for the 3D Poisson equation. Numer. Methods Partial Differ. Equ. **12**(2), 235–243 (1996)
23. Thomée, V.: Galerkin Finite Element Methods for Parabolic Problems. Springer, Berlin (2007)
24. Uzunca, M., et al.: Pricing European and American options under Heston model using discontinuous Galerkin finite elements. Tech. rep., arXiv:2004.14815 (2020)